2014 American Control Conference (ACC)
June 4-6, 2014. Portland, Oregon, USA

Grain Boundary Control in Colloidal Self-Assembly with Dynamic Programming

Xun Tang[1], Yuguang Yang[2], Michael A. Bevan[2], and Martha A. Grover[1,3]

Abstract— **We propose a Markov decision based dynamic programming method to manipulate the self-assembly of a quadrupole colloidal system for grain-boundary-free two-dimensional crystals. To construct the optimal control policy, we developed a Markov chain model, based on information extracted from a Langevin dynamics simulation model, which originated from a more complicated Brownian dynamics model. An infinite-horizon Markov decision process is defined, and the optimal control policy is solved with dynamic programming using policy iteration. Both the Markov chain Monte Carlo and the Langevin dynamics simulation results demonstrate that the control strategy is able to significantly accelerate the crystallization of a SiO_2 colloidal self-assembly process for a grain-boundary-free, highly ordered crystal. Future work will focus on implementation of the control policy on the Brownian dynamics simulation and the experiments.**

I. INTRODUCTION

Colloidal self-assembly refers to the process by which colloidal particles converge into an ordered structure with or without external interference. Periodically regular colloidal crystals, also called photonic crystals, have wide applications in various fields, including chemical and biological sensors [1], semiconductors [2], and photonic devices [3], due to their ability to manipulate the propagation of light. This unique feature of photonic crystals stimulated intense study on the techniques for its fabrication such as chemical stimuli-induced molecular interaction directed self-assembly, sedimentation, evaporation, adsorption, and external field directed self-assembly. Comprehensive literature reviews on the fabrication and applications of photonic crystals can be found in Ref. [4], [5], [6].

In spite of these many aforementioned techniques for photonic crystal fabrication, most self-assembling processes still suffer from defects, including vacancies and grain boundaries. Getting rid of these defects still remains one of the biggest challenges before the large-scale production of photonic crystals can be realized. In Ref. [7], the authors demonstrated that by periodically applying and removing the electric field during the self-assembly process, they were able to achieve a single-crystal monolayer in a microfluidic chamber. The authors' findings give a good example of using a time-varying external electric field to achieve single domain colloidal crystals. However, the crystals are not achieved in any optimized way, and there is no feedback.

[1] School of Chemical & Biomolecular Engineering, Georgia Institute of Technology, 311 Ferst Dr. NW, Atlanta, GA. 30332-0100.

[2] The Department of Chemical and Biomolecular Engineering, Johns Hopkins University, 221 Maryland Hall 3400 North Charles Street, Baltimore, MD 21218.

[3] Corresponding author: martha.grover@chbe.gatech.edu

In addition, using feedback control policies has emerged as a viable approach [8], [9], [10]. In Ref. [8], model predictive control was applied to a stochastic simulation of colloidal self-assembly to rapidly achieve a highly ordered crystalline state. In Ref. [9], dynamic programming was applied to a similar stochastic colloidal self-assembly process as in Ref. [8] for a rapid formation of a highly ordered crystalline state. Besides, in Ref. [10], Juarez and Bevan designed a proportional controller to enable the connection between the real-time sensing of this dynamic assembly process (via a crystalline order parameter named C_6) and the external tunable electric potential. They further demonstrated the development of the crystalline colloidal assembly from a fluid state under feedback control [10].

Recent study has shown the Markov chain model as a promising representative for micro scale processes [9], [11]. The robustness of a Markov decision process based control policy was demonstrated on a stochastic colloidal self-assembly process in Ref. [9] to produce a highly ordered colloidal crystal. In this paper, we introduce a Markov decision process based optimal control strategy to a SiO_2 self-assembly system for grain-boundary-free, and highly ordered two-dimensional crystals. In our past work [8], [9], we studied optimal control on a system with 174 particles with a one-dimensional Langevin model. This system did not exhibit persistent grain boundaries due to the small number of particles; however, in this study, 210 particles are used, and this leads to grain boundary formation and persistence during the assembly process. Fig. 1 depicts results from a Brownian dynamics simulation [13]. In Fig. 1(a) the system is in a fluid-like state, while in Fig. 1(c) the system is in the desired crystalline state. The system in Fig. 1(b) has a grain boundary, a condensed yet defected state.

In this paper, we constructed Markov chain models from a two-dimensional Langevin dynamics model, which originated from a Brownian dynamics simulation, to simulate the dynamics of the colloidal assembly process. Based on the Markov chain model, dynamic programming was used to design an optimal control policy. The purpose of this paper is to introduce a control strategy to robustly control the formation of a single domain colloidal crystal in a system where grain-boundary formation is prevalent. Detailed descriptions of the experimental system, the simulation models and the analysis of the control results are given in the following sections.

II. PROBLEM STATEMENT

In order to study the reliability of a Markov decision process based optimal controller for the colloidal self-assembly

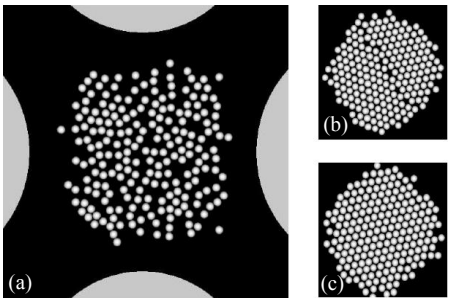

Fig. 1. (a) top view of dispersed colloidal particles in Brownian dynamics simulation; (b) colloidal ensemble with grain boundary; (c) colloidal ensemble without grain boundary

process, we consider a SiO_2 particle colloidal experiment developed by one of the authors (Bevan) [11]. In this system, 210 identical SiO_2 particles with a nominal size of 1.5 μm are suspended in deionized water in a container made of glass microscope cover slips (50 mm x 24 mm x 150 μm) [12]. Four separate, tunable 1 MHz AC electrode tips are attached to the edge of the container to generate a non-homogeneous electric field inside the container [12]. Details of the particle-particle and particle-field interaction forces have been studied and are simulated with a Brownian Dynamics (BD) model [13]. Previous studies have shown that by changing the magnitude of the voltage potential, the movement of the particles can be controlled, and thus the formation of the crystals [12]. Both laboratory experimental results and simulation results indicate that, for such a large colloidal system (with a particle number of 210), grain boundaries can be easily formed, thus posing an obstacle in achieving a single-domain, highly ordered crystal. Given these observations, we aim to develop a control policy with dynamic programming based on a Markov chain model, to rapidly form a grain-boundary-free SiO_2 crystal.

III. Theory and Methods

In order to more effectively study the dynamics of the colloidal assembly system considered in our study, and to more conveniently construct a control policy, we developed mathematical models for the system simulation and prediction. Based on the physical analysis of the interactions inside the system, we constructed a Brownian dynamics (BD) model which is able to accurately describe the experiments. However, considering its high computational time, we further developed a Langevin dynamics (LD) model to simplify the simulation. To enable the use of dynamic programming for our control policy, we further developed Markov chain models based the Langevin dynamics model.

In a colloidal assembly system, where the state variables are the coordinates of all the particles, the state space dimension can be prohibitively large. To reduce the state space dimension, we define an approximate system state using order parameters [14]. In the colloidal self-assembly system, a pair of order parameters is identified to describe the instantaneous state of the assembly process: ψ_6, which is a six-fold bond orientational order parameter, captures the occurrence of the grain boundary [12]; Rg, the radius of gyration, captures the condensation of the system [15]. A high Rg value together with a low ψ_6 value indicates a fluid-like state of the system, while a low Rg value together with a high ψ_6 value indicates a highly ordered, grain-boundary-free crystalline state. Therefore, the objective of the control is to achieve a state with the highest possible ψ_6 value and the lowest possible Rg value at the same time. These order parameters can be both theoretically calculated with a dynamics model and experimentally measured with a laboratory microscope, and this enables optimal control over both a simulation model and a laboratory experiment. With the help of a MATLAB program, Rg and ψ_6 values can be accurately calculated online every 0.125 s from the particle coordinates captured by a microscope in the laboratory experiments. The definitions of these two order parameters are specified in the following section.

Parameter	Value
$2a$ (nm)[a]	2920
κ^{-1} (nm)[b]	10
ψ (mV)[c]	-50.0
λ[d]	1.31
f_{CM}[e]	-0.4667
$\varepsilon_m/\varepsilon_0$[f]	78
d_g (μm)[g]	100

Table 1. Parameters for Brownian Dynamics simulation: (a) colloidal particle size, (b) Debye screening length, (c) particle and wall Stern potential, (d) peak voltage applied to electrodes, (e) Clausius-Mosotti factor for an AC field frequency at 1 MHz, (f) medium dielectric permittivity, (g) electrode spacing.

A. Brownian dynamics and Langevin dynamics model

In this paper, BD simulations in the canonical ensemble are performed for 210 colloidal particles for six different constant voltages: 0.3V, 0.4V, 0.45V, 0.5V, 0.7V, and 1V, where 'V' stands for the maximum possible voltage of 2 volts. The time step used to update the particle configuration is set as 0.1 ms. These simulations were run for 10^7 time steps with an initial equilibration time of 2×10^6 time steps. Configurations were stored every 10^3 time steps and used to calculate the order parameters Rg and ψ_6. The parameters used in the BD simulation are summarized in Table 1, while the detailed construction of the BD simulation is elaborated in Ref. [16].

Although the BD model describes the dynamics of the system accurately, it takes hours to finish even a single realization of the simulation. Considering the simplicity of Langevin dynamics and its success at microscopic-level crystallization simulation [7], [8], [17], we further developed an LD model to shorten the computational time. The Langevin equation of motion specifying the evolution of the coordinate vector in order parameter space is given as:

$$\frac{\partial x}{\partial t} = -\beta D(x)\cdot\bigtriangledown W(x) + \bigtriangledown\cdot D(x) + \zeta(x,t) \qquad (1)$$

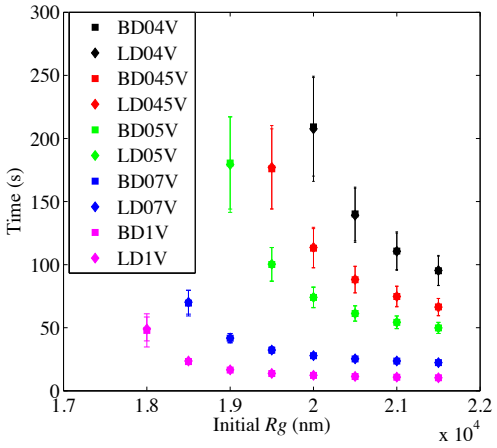

Fig. 2. 1000-realization averaged BD and LD mean first passage times starting from different Rg values under different constant voltages

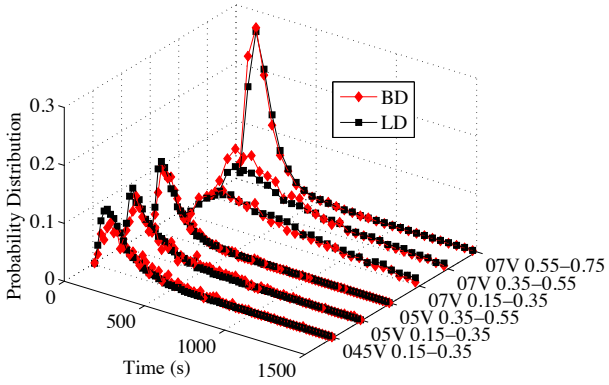

Fig. 3. 1000-realization averaged BD and LD mean first passage time distributions starting from different ψ_6 values under different constant voltages

where $x = (Rg, \psi_6)$ is the coordinate vector, tensor field $D(x)$ and scalar potential field $W(x)$ are diffusivity landscape (DL) and free energy landscape (FEL) which depend on the coordinates. ζ is the random noise variable with zero mean and variance $\langle \zeta_i(x,t)\zeta_j(x,t')\rangle = 2D_{ij}(x)\delta(t-t')$, as required by the Einstein relation, where i, j stand for Rg and ψ_6 respectively. $\bigtriangledown$ is a gradient operator, and $\bigtriangledown\cdot$ is a divergence operator. The DL and FEL, as the input quantities of the LD equation, are derived from particle scale Brownian dynamics via the linear fitting method [18]. To evaluate the accuracy of the LD simulation model, we compared the mean first passage time of both order parameters, under several constant voltages, against the results from the BD simulation.

Fig. 2 shows the comparison of the time needed for the system to decrease by 1000 nm in the Rg coordinate, from different initial points. In Fig. 2, the mean first passage time under 0.4V from Brownian dynamics is labeled as 'BD04V', and that from Langevin dynamics is labeled as 'LD04V', etc. The error bar in the plots shows the standard deviation at each point. The comparison demonstrates a good agreement between the LD and the BD model.

Fig. 3 shows the comparison of the distribution of the time needed for the system to increase by 0.2 in the ψ_6 coordinate, from different initial points. For example, the distribution labeled as '045V 0.15–0.35' denotes the time distribution of a 1000-realization-simulation for the system to travel 0.2 in ψ_6 from $\psi_6 = 0.15$ to $\psi_6 = 0.35$ under a constant voltage of 0.45V. With these mean first passage time comparisons, we validate the accuracy of our Langevin dynamics.

B. Markov Chain Model

Considering the construction of the simulation model described in the above sections, together with the observation from the laboratory experiments, the state of the assembly process at each instant depends only on the previous system state and the voltage used at that state. Therefore, we can use a parameterized-time-independent Markov chain model to simulate the system, and at the same time to enable the development of an optimal control policy.

A first step in building a Markov chain model is to define the discrete state space S, transition matrix P_a, and the discrete actuation space A. In this SiO_2 colloidal self-assembly system, we discretize the order parameter ψ_6 into $N_1 = 40$ evenly spaced grid cells, with $\psi_6 \in [0,1]$; and order parameter Rg into $N_2 = 156$ evenly spaced grid cells, with $Rg \in [16200, 24000]$. Therefore, the final state space is discretized into $N = N_1 \times N_2$ grid cells. The choice of the bounds on these two order parameters are based on the effective space that can be visited by the system according to the free energy landscape analysis. The actuation space A is defined as $A = \{0.3V, 0.4V, 0.45V, 0.5V, 0.7V, 1.0V\}$.

The transition matrix P_a contains the probabilities $p_{a_{ij}}$ for the system to be in state j, given the current state of i and action of a after a time step of Δt. The Δt value plays a significant role in determining the accuracy of the Markov chain model. By doing in-depth mean first passage time analysis for different Δt values, $\Delta t = 10$ s is found to give an accurate Markov chain model to capture the dynamics of the system, and is used in all the following calculations. Given the Δt value, the probability transition matrix P_a is constructed by running 50 independent Langevin dynamics simulations at each of 2070 distinct initial points. These initial points are chosen to cover the effective space of the colloidal system. With all the LD simulations, the $N \times N$ transition matrix P_a for each of the six actuators was achieved. A model characterized by the pair $\{S, P_a\}$ is referred to as a finite-state Markov chain model [19].

C. Markov Decision Process Based Dynamic Programming

A Markov decision process (MDP) is characterized by $\{T, S, A, P_a\}$ [20], where S, A, and P_a are defined as in the previous section. T is the collection of the discrete time epoch k. If T is finite, the MDP is called finite-horizon MDP, and it is called infinite-horizon MDP if T is infinite. Given the fact that an optimal control policy for a discounted infinite-horizon MDP is time-independent [18], we decided to adopt a discounted infinite-horizon MDP in our system for

the control policy. The control policy is solved with dynamic programming using policy iteration.

In infinite-horizon MDP, the optimization is achieved over an infinite number of time steps, and the objective function for an infinite-horizon MDP is defined as:

$$J_a(x) = E\left\{\sum_{k=0}^{\infty} \gamma^k R(x_k, a_k)\right\} \tag{2}$$

where E is the expectation operator, $a \in A$ is the control action, $x \in S$ is the discrete system state, $k \in T$ is the discrete time instant, and $\gamma \in (0,1)$ is the discount factor introduced to ensure the convergence of the optimization [21]. $R(x,a)$ is the one-stage reward function obtained when the system is in state x and a control action a is taken according to the optimality criterion, and it follows that $R(x,a) : S \times A \to \mathbb{R}$. The optimal value function and the optimal policy $a^*(x) \in A$ are defined as:

$$\begin{aligned} J^*(x) &= \sup_{a \in A} J_a(x) \\ a^*(x) &= \arg\{\sup_{a \in A} J_a(x)\} = \arg J^*(x) \end{aligned} \tag{3}$$

In our particular system, the one-stage-reward function is defined as:

$$R(x_k, a_k) = {\psi_6}^2 \tag{4}$$

The optimal control policy is obtained by solving for the input a trajectory that maximizes the sum of this one-stage-reward function over an infinite time horizon via policy iteration with discount factor $\gamma = 0.99$. The design of the reward function is aimed to achieve the highest possible ψ_6 value, which corresponds to a highly ordered, single domain crystalline state of the system. Rg is not included in the reward function, because it is impossible to achieve a high value of ψ_6 without a low value of Rg.

IV. RESULT AND DISCUSSION

Based on the methods described in Section III, we constructed six Markov chain models for each of the six actuation voltages: 0.3V, 0.4V, 0.45V, 0.5V, 0.7V, and 1V. To evaluate the accuracy of these models, in Fig. 4, we compared the 300-second uncontrolled simulation results under each of these six voltages for both the Markov chain model and the LD model. The legend 'MCMC', and 'LD' stands for Markov chain Monte Carlo simulation and Langevin dynamics simulation respectively. '03V' through '1V' denotes the voltage under which the simulations are conducted. All these trajectories are averages over 1000 independent simulations from the same initial point of $Rg = 20000$ nm, and $\psi_6 = 0.1$, which corresponds to a fluid-like state of the system. According to this comparison, although the Markov chain model tends to overpredict the dynamics in the aspect of ψ_6, the differences are slight. One noticeable phenomenon in these uncontrolled trajectories is, as the magnitude of the voltage increases, the system would reach a better, more crystalline state, which is defined by a high ψ_6 value and a low Rg value. Intuitively, one would expect to use the highest possible voltage all the time to most efficiently form

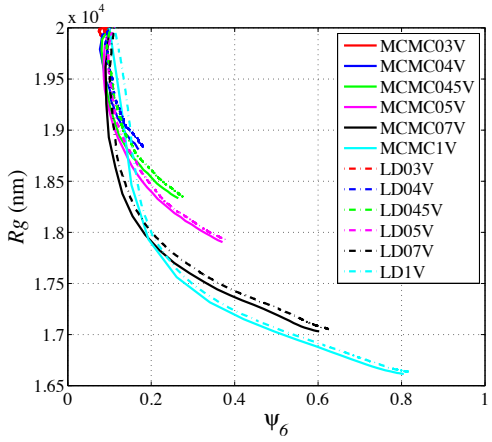

Fig. 4. Comparison between 1000-realization averaged MCMC and LD simulation order parameter trajectories for different constant input a from a system without the optimal control policy

the crystals. However, experimental results show that under a high potential, like 0.7V and 1V, the particles are pushed together too quickly, which leaves less time for the system to self-correct for defects. Once the system gets stuck in a disordered state, it will take a long time for the system to relax through self-corrections, and this makes it impractical for a real world production. Therefore, using a high voltage all the time might not be the optimal policy.

With these six Markov chain models, a time-independent optimal control policy was developed using dynamic programming. Fig. 5 shows the control policy in a two-dimensional plot. The numbers in the color bar stand for the control actions in an increasing order, where 1 stands for voltage 0.3V, and 6 stands for voltage 1V. This policy is interpreted as a look-up table. To use it, for example, when the system is in state of $Rg = 1.8 \times 10^4$ nm and $\psi_6 = 0.4$, the voltage of 1V should be used, which is colored as red and labeled as 6 in Fig. 5. In the control policy, the highest voltage of 1V is optimal in most of the effective space; this observation meets the expectation in Fig. 4 that a high voltage would result in a higher crystalline state than a lower voltage. However, one important point in the control policy is the use of lower voltages in the region of $Rg \leq 1.7 \times 10^4$ nm and ψ_6 around 0.6. These lower voltages are used to give the system long enough relaxation time for self-corrections in order to avoid getting stuck in the disordered state.

The implementations of the control policy onto both the Markov chain model and the Langevin dynamics simulation demonstrate that the control policy shown in Fig. 5 is able to yield a better crystalline state than an uncontrolled process. Detailed comparison results are given in Fig. 6. In Fig. 6, we only showed the LD uncontrolled trajectories for comparison, considering the agreement between the uncontrolled LD and MCMC simulations illustrated in Fig. 4.

Fig. 6 shows the comparison of 1000-realization averaged controlled Langevin dynamics (LDcontrolled) and Markov chain Monte Carlo (MCcontrolled) simulations against the uncontrolled Langevin dynamics (LD03V through LD1V)

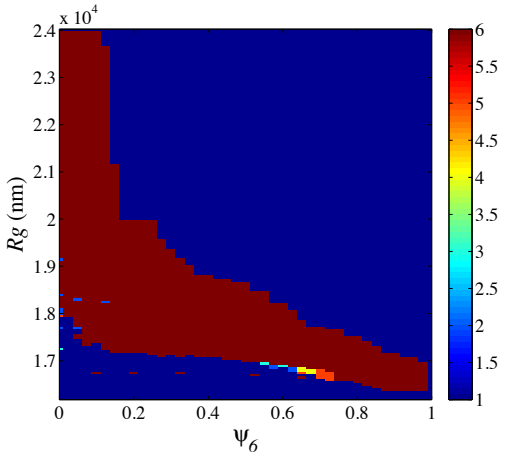

Fig. 5. Optimal control policy computed using Markov decision based dynamic programming

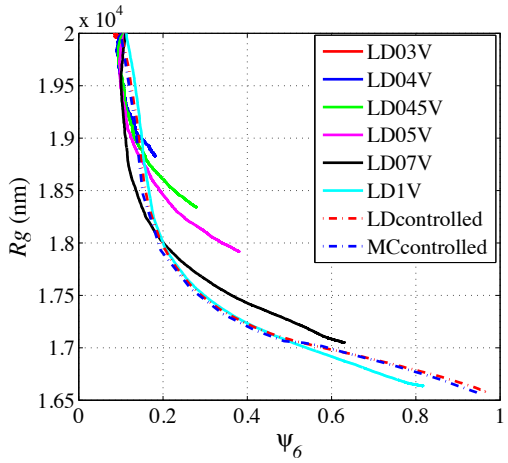

Fig. 6. Comparison between 1000-realization averaged order parameter trajectories with and without optimal control policy

results over 300 seconds. All the trajectories are averages over 1000 independent realizations starting from the same initial point of $Rg = 20000$ nm and $\psi_6 = 0.1$.

From the comparison, we conclude the effectiveness of the control policy by noticing the system reached ψ_6 of around 0.95 and Rg of around 1.65×10^4 nm after 300 seconds under the control. The highest possible ψ_6 value that can be achieved without control is around 0.8 under 1V. The comparison reveals an obvious divergence between the controlled trajectory and the 1V uncontrolled trajectory around the point of $\psi_6 = 0.5$ and Rg around 1.7×10^4 nm due to the use of 0.3V. Because of this use of a low voltage, the system enjoys a boost in ψ_6 by correcting defects introduced by the high voltages. Therefore it leads to a higher final ψ_6 value after 300 seconds of simulation. All these observations meet the expectation that high voltages should be used most of the time according to Fig. 5, while low or intermediate voltages should also be used to provide corrections during the process. Besides, the controlled Markov chain Monte Carlo simulation and the controlled Langevin dynamics simulation demonstrate a high similarity with each other, which further confirms the accuracy of the Markov chain model in approximating the LD model.

In addition, the evolution of the order parameters over time for both the Markov chain Monte Carlo and the Langevin dynamics simulations are investigated for a better understanding of the performance with respect to time. Results are summarized in Fig. 7.

Fig. 7 shows the evolution of the order parameters over time, with the system started from a fluid-like state with a low ψ_6 value and a high Rg value, and developed into a highly ordered crystalline state with a high ψ_6 value and a low Rg value after 300 seconds of simulation. In Fig. 7, all these four order parameter trajectories are averaged over 1000 independent realizations. From this figure, we can see that both Rg and ψ_6 reach a steady state after about 250 seconds of simulation in the LD model. While ψ_6 achieves its steady state after about 150 seconds, Rg stabilizes after about

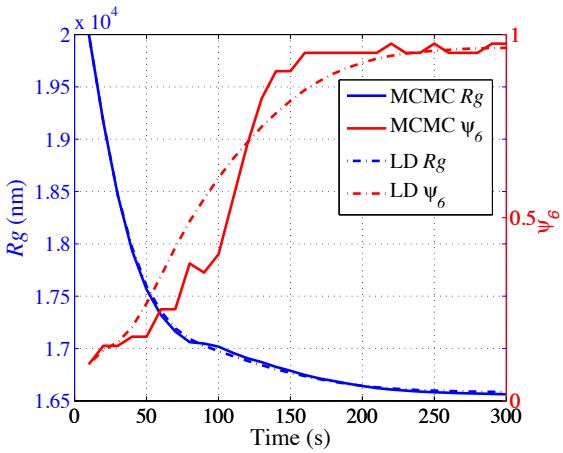

Fig. 7. 1000-realization averaged MCMC and LD simulation: order parameter evolution over time, under the optimal policy in Fig. 5

250 seconds in the MCMC simulation. These observations indicate the actual time needed for the system to reach a highly ordered, grain-boundary-free crystalline state is shorter than 300 seconds under the control policy.

Besides, the analysis of the averaged optimized control actions demonstrates that the use of high voltages for most of the time together with the use of low or intermediate voltages at times of around 70 seconds is able to give a better crystalline state. Both the optimized voltage trajectories from Markov chain Monte Carlo simulation (solid red line) and Langevin dynamics simulation (solid blue line) are summarized in Fig. 8.

Fig. 8 shows the 1000-realization optimized control action for both the Markov chain model and the LD model over 300 seconds of simulation. A similar trend can be observed in both of these two trajectories: at the beginning of the simulation, the highest voltage 1V was used to give the system a strong momentum to initialize the crystallization. However, when the system evolves to Rg of 1.7×10^4 nm and ψ_6 around 0.4, a low voltage is sometimes used to

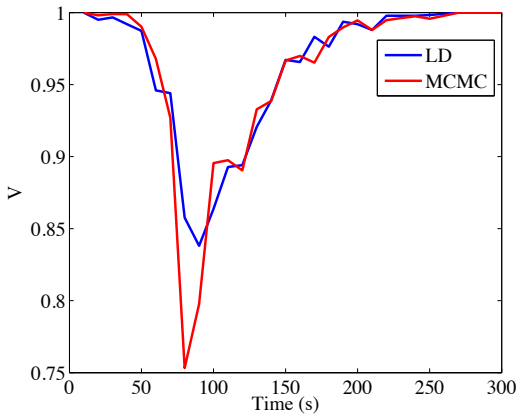

Fig. 8. 1000-realization averaged MCMC and LD simulation: input voltage evolution in time, under the optimal policy

correct defects that are caused by the strong electric forces induced by applying a high voltage. This strategy is well demonstrated in the control policy given in Fig. 5. Once the defects get resolved, the system chooses to use higher and higher voltages towards the end of the simulation to further speed up the process. The use of high voltage in the end is also justified physically, that a strong electric force is better able to maintain the system in a highly ordered state than a lower voltage. However, the optimized control policy trajectories from the MCMC and the LD simulation shows a noticeable difference between each other. This is due to the fact that the number of the realizations that used a non-trivial control policy (a control that is not using a constant voltage V) differs in the two sets of 1000 realization simulations. Specifically, 361 out of 1000 realizations used a non-trivial control policy in the LD simulation, while 631 out 1000 realizations used a non-trivial control policy in the MCMC simulation. This observation further demonstrates that using a highest constant voltage throughout the simulation does not necessarily guarantee an optimal result, in both the MCMC and the LD simulation.

The ultimate goal of this work is to feasibly produce grain-boundary-free crystals in the lab with the control policy shown in this paper. Given the simulation results, our next step is to apply the control policy in the BD simulation and in the laboratory experiment for the production of single domain, defect-free SiO_2 colloidal crystals.

V. CONCLUSIONS

Using Markov decision process based dynamic programming for a SiO_2 colloidal self-assembly process, we are able to achieve a single domain, highly ordered colloidal crystal in simulations. From all the analysis of the controlled and uncontrolled MCMC and LD simulation results, we conclude that a Markov chain model is suitable for simulating the dynamics of the stochastic self-assembly system. We further conclude that the controlled system gives significantly better results than the uncontrolled system, and a grain-boundary-free crystalline state can be achieved within about 250 seconds of simulation time under the control. Given the required policy updating time, $\Delta t = 10$ s, and the laboratory order parameter calculation time, 0.125 s, the in-lab control experiments are practical and are ongoing.

ACKNOWLEDGMENT

Acknowledgment is made to the National Science Foundation for support of this research, through collaborative grant Grant #1124678 (Grover) and #1124648 (Bevan) through the Cyber-Enabled Discovery and Innovation program.

REFERENCES

[1] Q.-H. Wei, D. M. Cupid and X. L. Wu, Controlled assembly of two-dimensional colloidal crystals, Applied Phys. Letters, vol. 77 pp. 1641 Sep. 2000.
[2] O. D. Velev and A. M. Lenhoff, Colloidal crystals as templates for porous materials, Curr. Opin. Colloid Interface Sci. vol. 5 pp. 56, 2000.
[3] S. O. Lumsdon, E. W. Kaler and O. D. Velev, Two-dimensional crystallization of microspheres by a coplanar AC electric field, Langmuir, vol. 20 pp. 2108-2116 Jan. 2004.
[4] M. Grzelczak, J. Vermant, E. M. Furst and L.M. Liz-Marzán, Directed self-assembly of nanoparticles, ACS Nano, vol. 4 pp. 3591-3605 Jun. 2010.
[5] K. A. Arpin, A. Mihi, H. T. Johnson, A. J. Baca, J. A. Rogers, J. A. Lewis, and P. V. Braun, Multidimensional architectures for functional optical devices, Adv. Mater., vol. 22 pp. 1084-1101 Feb. 2010.
[6] O. D. Velev and S. Gupta, Materials fabricated by micro- and nanoparticle assembly – the challenging path from science to engineering, Adv. Mater., vol. 21 pp. 1897-1905 Feb. 2009.
[7] S. Kim, R. Asmatulu, H. L. Marcus and F. Papadimitrakopoulos, Dielectrophoretic assembly of grain-boundary-free 2D colloidal single crystals, J. Colloid and Interface Sci., vol. 354 pp. 448-454 Nov. 2010.
[8] X. Tang, Y. Xue, and M. A. Grover, Colloidal self-assembly with model predictive control, Proceedings of the 2013 American Control Conference Jun. 2013.
[9] Y. Xue, D. J. Beltran-Villegas, X. Tang, M. A. Bevan and M. A. Grover, Optimal design of colloidal self-assembly process, IEEE Trans. on Control Systems Technology, 2014, doi: 10.1109/TCST.2013.2296700.
[10] J. J. Juárez and M. A. Bevan, Feedback controlled colloidal self-assembly, Adv. Funct. Mater., vol. 22 pp. 3833-3839 Sep. 2012.
[11] A. Banerjee, A. Pomerance, W. Losert and S. Gupta, Developing a stochastic dynamic programming framework for optical tweezer based automated particle transport operations, IEEE Trans. on Automation Science and Engineering, vol. 7 pp. 218-227 Apr. 2010.
[12] J. J. Juárez, S. E. Feicht and M. A. Bevan, Electric field mediated assembly of three dimensional equilibrium colloidal crystals, Soft Matter, vol. 8 pp. 94-103, 2012.
[13] J. J. Juárez and M. A. Bevan, Interactions and microstructures in electric field mediated colloidal assembly, J. Chem. Phys., vol. 131 pp. 134704 Oct. 2009.
[14] D. J. Beltran-Villegas, R. Sehgal, D. M. Maroudas, D. M. Ford and M. A. Bevan, Fokker-Planck analysis of separation dependent potentials and diffusion coefficients in simulated microscopy experiments, J. Chem. Phys. vol. 123 pp. 044707 Jan. 2010.
[15] D. J. Beltran-Villegas and M. A. Bevan, Free energy landscapes for colloidal crystal assembly, Soft Matter vol. 7 pp. 3280-3285 Feb. 2011.
[16] S. G. Anekal and M. A. Bevan, Interpretation of conservative forces from Stokesian dynamic simulations of interfacial and confined colloids, J. Chem. Phys., vol. 112 pp. 34903 Jan. 2005.
[17] C. Liu and M. Muthukumar, Langevin dynamics simulations of early-stage polymer nucleation and crystallization, J. Chem. Phys., vol. 109 pp. 2536 Aug. 1998.
[18] D. I. Kopelevich, A. Z. Panagiotopoulos and I. G. Kevrekidis, Coarse-grained kinetic computations for rare events: application to micelle formation, J. Chem. Phys., vol. 122 pp. 044908 Jan. 2005.
[19] D. P. Bertsekas, Dynamic Programming and Optimal Control. Nashua, NH: Athena Scientific, 2005.
[20] M. L. Puterman, Markov Decision Processes Discrete Stochastic Dynamic Programming. Hoboken, NJ: Wiley-Interscience, 2005.
[21] H. Chang, M. Fu, J. Hu and S. Marcus, Simulation-Based Algorithms for Markov Decision Processes. New York, NY: Springer, 1989.